Temperature Dependence of the Q_y Resonance Raman Spectra of Bacteriochlorophylls, the Primary Electron Donor, and Bacteriopheophytins in the Bacterial Photosynthetic Reaction Center†

Nerine J. Cherepy,‡,§ Andrew P. Shreve,‡,|| Laura J. Moore,⊥ Steven G. Boxer,⊥ and Richard A. Mathies*,‡

Department of Chemistry, University of California, Berkeley, California 94720, and Department of Chemistry, Stanford University, Stanford, California 94305

Received January 3, 1997; Revised Manuscript Received April 9, 1997⊗

ABSTRACT: Q_y-excited resonance Raman spectra of the accessory bacteriochlorophylls (B), the bacteriopheophytins (H), and the primary electron donor (P) in the bacterial photosynthetic reaction center (RC) of *Rhodobacter sphaeroides* have been obtained at 95 and 278 K. Frequency and intensity differences are observed in the low-frequency region of the P vibrational spectrum when the sample is cooled from 278 to 95 K. The B and H spectra exhibit minimal changes of frequencies and relative intensities as a function of temperature. The mode patterns in the Raman spectra of B and H differ very little from Raman spectra of the chromophores *in vitro*. The Raman scattering cross sections of B and H are 6−7 times larger than those for analogous modes of P at 278 K. The cross sections of B and of H are 3−4 times larger at 95 K than at 278 K, while the cross sections of P are approximately constant with temperature. The temperature dependence of the Raman cross sections for B and H suggests that pure dephasing arising from coupling to low-frequency solvent/protein modes is important in the damping of their excited states. The weak Raman cross sections of the special pair suggest that the excited state of P is damped by very rapid (<30 fs) electronic relaxation processes. These resonance Raman spectra provide information for developing multimode vibronic models of the excited-state structure and dynamics of the chromophores in the RC.

The photophysical properties of the chromophores in the photosynthetic reaction center (RC)[1] have been extensively studied with the goal of understanding how they mediate efficient electron transfer reaction across the photosynthetic membrane (Boxer et al., 1989; Rees et al., 1989; Fleming & van Grondelle, 1994; Friesner & Won, 1989; Kirmaier & Holten, 1987). The bacterial reaction center of *Rhodobacter sphaeroides* has an approximate C_2 axis of symmetry about which lies a bacteriochlorophyll (BChl) dimer P, two monomeric BChls called B, and two bacteriopheophytin (BPheo) molecules called H. The lowest energy Q_y electronic transitions of the P, B, and H chromophores lie in the near-infrared, with peaks at room temperature near 860, 800, and 760 nm, respectively (Figure 1). Charge separation is complete between the special pair and a bacteriopheophytin within about 3 ps at room temperature and in about half that time at 100 K. Excitation of B or H leads to ultrafast (100−200 fs) energy transfer to P, although the details of the excited-state dynamics in B are as yet unresolved (Jia et al., 1995; Martin et al., 1986; Stanley et al., 1996). The electronic transitions comprising the near-infrared absorption bands of the RC need to be better characterized and the nature of their vibronic coupling determined in order to better understand the rapid and efficient photochemistry in the RC.

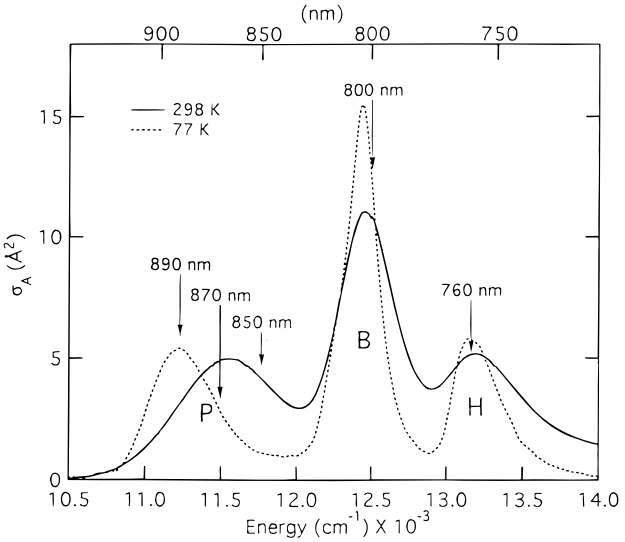

FIGURE 1: Near-IR absorption spectra of *Rb. sphaeroides* reaction centers at 298 and 77 K. Excitation wavelengths of 890, 870, and 850 nm were used to acquire the Raman spectra of P while 800 and 760 nm excitation were used to acquire the B and H spectra.

Resonance Raman spectra and their temperature dependence can provide insight into the electronic dynamics and reveal the normal coordinates along which the chromophores distort when electronically excited. Comparisons with model

† This work was funded by NSF Grant CHE 94-19714 to R.A.M. A.P.S. was supported by a National Institutes of Health Postdoctoral Fellowship (GM 14298). S.G.B. thanks the National Science Foundation Biophysics Program for its support.

* Author to whom correspondence should be addressed.

‡ University of California at Berkeley.

§ Current address: Department of Chemistry, University of California, Santa Cruz, CA 95064.

|| Current address: Los Alamos National Laboratory, CST-4, MS G755, Los Alamos, NM 87545.

⊥ Stanford University.

⊗ Abstract published in *Advance ACS Abstracts,* June 15, 1997.

[1] Abbreviations: RC, reaction center; BChl, bacteriochlorophyll; BPheo, bacteriopheophytin; SERDS, shifted excitation Raman difference spectroscopy; FT, Fourier transform; OD, optical density.

S0006-2960(97)00024-X CCC: $14.00

compound Raman spectra and other techniques such as site-selective emission and hole-burning spectra are also useful for characterizing the role of the protein in tuning the chromophores for their specific functions in the RC. The modes observed in a resonance Raman spectrum are strongly coupled to the resonant electronic absorption. Thus, the Raman spectrum provides specific information about the structure, excited-state structural relaxation, and environment of a bound chromophore. Although Raman frequencies and relative intensities of high-frequency modes typically do not change significantly with temperature, changes in absolute Raman cross sections can provide information about the excited−state dynamics. A self-consistent model of the absorption spectrum and the excitation-wavelength-dependent resonance Raman cross sections can then be used to develop a multidimensional excited-state potential energy surface model and a description of the electronic state relaxation rates, as has been demonstrated for other photobiological systems (Loppnow & Mathies, 1988; Morikis et al., 1991; Myers et al., 1983; Phillips & Myers, 1991; Sue & Mukamel, 1988).

Here we present resonance Raman spectra of B, H, and P at both 95 and 278 K with excitation on resonance with their Q_y transitions. Our previous studies at 278 K of the B and P bands identified many common modes as well as some unique modes for each chromophore (Cherepy et al., 1994; Shreve et al., 1991). We have now obtained spectra at 95 and 278 K exciting in the Q_y transitions of B, H, and P. We have also quantified the Raman scattering strength of each chromophore by using an internal standard. While the Raman cross sections of P are approximately independent of temperature, the scattering cross sections of B and H are found to be dramatically temperature dependent. The multimode information provided by the Raman spectra and their analysis will aid in the interpretation of other vibronic spectroscopic experiments such as the photochemical hole burning of P (Johnson et al., 1989; Klevanik et al., 1988; Meech et al., 1985; Middendorf et al., 1991) and the oscillations observed in femtosecond time-resolved stimulated and spontaneous emission from P* (Stanley & Boxer, 1995; Vos et al., 1991, 1993).

EXPERIMENTAL SECTION

RCs were isolated from wild-type and the R-26 mutant of *Rb. sphaeroides* as described previously (Okamura et al., 1975; Schenck et al., 1982). Q_A-depleted RCs exhibit faster recombination to the ground state, but they are unstable when flowed at high speed at ambient temperature. Therefore, Q_A-containing RCs suspended in buffered detergent solution (0.025% LDAO, 10 mM TRIS, pH 8) or in a solution of buffered detergent and 50% ethylene glycol were used to acquire all spectra at 278 K. Experiments at 95 K were performed on Q_A-depleted RCs. For the B and H spectra at 95 K, R-26 RCs were used, while for the P spectra, wild-type RCs were employed.[2] In order to produce optically clear glasses, RCs were suspended in buffered detergent and 60% glycerol, or in a mixture of buffer, 30% glycerol and 50% ethylene glycol.

[2] Wild-type RCs were used in these experiments because triplet-state P, which would be generated under these conditions, is long-lived in the carotenoidless mutant and may absorb in the same spectral region as the initial ground-to-excited state transition of P. We have verified that wild-type and R-26 RCs have the same P Raman spectrum at 278 K, and we assume that their 95 K spectra are also the same.

A detailed presentation of the methodology used in deriving the absolute Raman cross sections from comparison of the RC Raman scattering intensities with the ethylene glycol scattering will be found in Cherepy et al. (1997a). Raman scattering from the 864 cm^{-1} mode of ethylene glycol can be observed when the RC concentration is reduced enough to compensate for the resonance enhancement. For quantitative work, the intensity of the strong 730 cm^{-1} RC mode was measured relative to that of the 864 cm^{-1} standard, and the concentrations used were typically $OD_{800nm,298K} \approx 0.15$/cm for 800 nm excitation at 278 K, $OD_{800nm,298K} \approx 0.03$/cm for 800 nm excitation at 95 K, $OD_{800nm,298K} \approx 1.5$/cm for measurements with 850 nm excitation at 278 K, and $OD_{800nm,298K} \approx 1.2$/cm for 870 nm excitation at 95 K. The full spectra were then obtained separately using a more concentrated solution (OD $\approx$ 3.0/cm) without ethylene glycol.

Resonance Raman spectra acquired at 278 K of rapidly flowing solutions of RCs were obtained as described previously (Cherepy et al., 1994, 1995; Shreve et al., 1991). Excitation powers at all temperatures and wavelengths were typically 5 mW for measuring the full spectra and 2 mW for measuring the relative intensities in the 50% ethylene glycol solution. The 95 K experiments employed a Harney−Miller low-temperature cell, in which the 1 mm i.d. sample capillary is cooled by circulating cold N_2 gas through the cell. Raman spectra were recorded with a cooled CCD detector (LN/CCD-1152, Princeton Instruments) coupled to a subtractive-dispersion, double spectrograph (Mathies & Yu, 1978) equipped with 600 g/mm grating and one 1200 g/mm grating, both blazed at 750 nm (10 cm^{-1} entrance slit). We have employed the shifted-excitation Raman difference technique described in our earlier work (Cherepy et al., 1994, 1995, 1996; Shreve et al., 1991, 1992) to acquire Raman spectra in the presence of the intrinsic fluorescence background from P* (Zankel et al., 1968). All spectra were corrected for the wavelength dependence of the detection system by use of a standard lamp. Frequency calibration for the spectra is accurate to $\pm$ 3 cm^{-1}.

Since the laser excitation may result in bleaching of the P band, precautions must be taken to quantitatively measure resonance Raman cross sections. Measurements of the Raman intensities of P were made with 2−10 mW excitation, depending on the extinction coefficient at the resonant wavelength. Since Q_A-containing RCs have a $P^+Q_A^- \rightarrow PQ_A$ recombination time of about 100 ms, which is long compared to the transit time of the sample through the beam ($\sim$25 μs), a correction for bleaching may be required. This correction was applied to P cross sections with excitation between 830 and 910 nm. The exact correction applied to each measurement varies with excitation wavelength and with the power used for each measurement.

The photoalteration parameter F for a cylindrically focused beam is defined as (Mathies et al., 1976)

$$F = \sigma_A \Phi P / a v \qquad (1)$$

where σ_A is the absorption cross section (σ = 4.21 Å^2 at 850 nm and 278 K), Φ, the photochemical quantum yield, is $\sim$1 for the special pair, P is the photon flux in photons per second, a is the beam dimension perpendicular to the flow direction (0.1 cm in a 0.1 cm i.d. capillary), and v is the linear flow velocity (200 cm/s).

Typical F values are $\sim$0.10 $mW^{-1} \times P$ where P is the excitation power in mW. The effective fraction of photo-

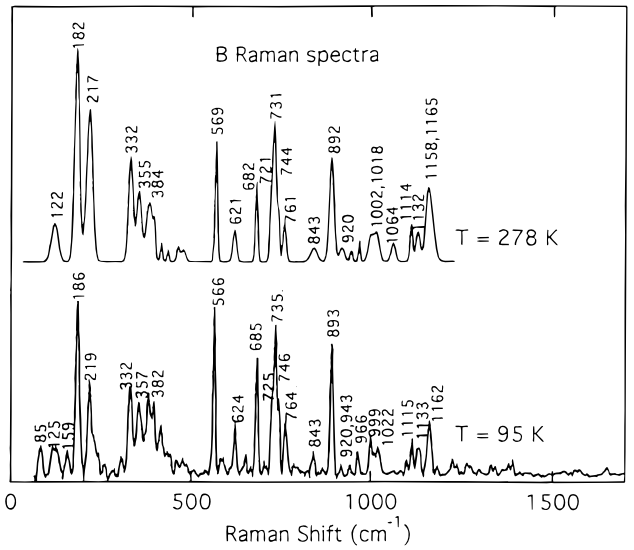

FIGURE 2: (Top) Raman spectrum of B at 278 K obtained using 800 nm excitation and the SERDS technique (T = 278 K, P = 5−8 mW). (Bottom) Raman spectrum of B at 95 K obtained using 800 nm excitation (P = 5−8 mW). Spectra adapted from Cherepy et al. (1997a).

altered molecules sensed by the Raman experiment, f, is determined by the photoalteration parameter, F:

$$f = [1 - (1/F)(1 - \exp(-F))] \quad (2)$$

The observed relative Raman cross sections were multiplied by $1/(1 - f)$ to correct for bleaching of the sample as it passed through the excitation beam. For example, the ratio of the intensity of the 730 cm^{-1} RC mode to the 864 cm^{-1} ethylene glycol mode acquired with an excitation power of 2 mW, would be multiplied by a factor of 1.15 to obtain the actual relative intensity.

Q_A-depleted R-26 RCs have a recombination time of ∼1 μs and were used to acquire the B and H spectra at 95 K; however, it was found that the Raman intensities of B and H at 95 and 278 K were independent of the oxidation state of P and whether Q_A-containing or Q_A-depleted RCs were used. For the low-temperature experiments on P, Q_A-depleted wild-type RCs were used because they have a ground-state recombination time of 70 ns. This recombination time is about 1000 times faster than the mean time between absorptions (τ_a) of 80 μs, which is given by

$$\tau_a = A/\sigma P \quad (3)$$

where σ is the absorption cross section (∼2.9 $Å^2$/molecule at 870 nm, 77 K), P is the laser power in photons per second (typically ∼2 × 10^{16} photons/s at 870 nm and 5 mW), and A is the excitation area (∼5 × 10^{-4} cm^2). Due to the fast recombination of Q_A-depleted wild-type RCs, it was unnecessary to correct for photobleaching of the stationary sample used for measuring the cross sections at 95 K.

RESULTS

The Raman spectra of B obtained with 800 nm excitation at 278 and 95 K from Cherepy et al. (1997a) are presented in Figure 2 for reference. Table 1 (Supporting Information) summarizes the Raman frequencies and intensities of B. The 278 and 95 K spectra exhibit only a few minor differences. The mode at 85 cm^{-1} which is clearly resolved at 95 K may also be present as a feature at ∼80 cm^{-1} in the 278 K spectrum, but was not fit in the SERDS spectrum due to the increased noise in this region. The 182 cm^{-1} mode in the 278 K spectrum appears to split into the 159 and 186 cm^{-1} modes at 95 K.

The resonance Raman spectra of H at 278 and 95 K, taken with 760 nm excitation, are presented in Figure 3, panels A and B, respectively. These SERDS spectra of H are more difficult to fit than the B and P spectra due to the presence of more overlapping modes. As a control, the direct-detected spectrum of H was obtained at 95 K over the 500−1000 cm^{-1} range (not shown). Despite the difficulties in flat-field correcting the direct spectrum, the data agree very well with the SERDS spectra. Since only the mid-frequency region of the H spectrum was acquired at 278 K, we are only able to examine the temperature dependence of modes in the 500−1250 cm^{-1} range. Several of the peaks observed at 278 K split into two or more peaks at 95 K, probably due to narrowing of the Raman line widths at lower temperature. For example, the 765 cm^{-1} peak is resolved into the 753 and 773 cm^{-1} modes, the 844 cm^{-1} peak splits into peaks at 839, 845, and 852 cm^{-1}, and the 972 cm^{-1} band produces the 969 and 980 cm^{-1} modes. The relative intensities of the H modes and their frequencies are summarized in Table 2 (Supporting Information).

Comparison of the resonance Raman spectra of H with the room-temperature BPheo Fourier Transform (FT) Raman spectra (Mattioli et al., 1993) and the 5 K site-selection emission spectra (Renge et al., 1987) of BPheo is useful in identifying BPheo bands and in revealing how the chromophore is perturbed by protein binding. Some of the modes in the Raman spectra acquired with excitation in the H absorption at 760 nm originate from resonance enhancement from the 0−1 vibronic transition of B. Comparisons of the calculated Raman excitation profiles for the B modes with the vibrational spectra of BPheo allow us to identify the B modes in the H spectra (see Table 2, Supporting Information). The modes of B, which show strongest enhancement with 760 nm excitation, are in the 500−900 cm^{-1} range (Cherepy et al., 1997a). Thus, we predict that the B modes at 682, 721, 731, 744, 892, and 1018 cm^{-1} underlie or may be the sole source of the bands in the 760 nm H spectrum at 685, 724, 735, 748, 897, and 1023 cm^{-1}. This is consistent with the observation that neither the FT Raman spectrum nor the site-selection emission spectrum of BPheo exhibits strong modes at these frequencies.

The resonance Raman spectra of P at 278 K (850 nm excitation) and at 95 K (870 nm excitation) are presented in Figure 4. Table 3 (Supporting Information) lists experimental mode frequencies and relative intensities for P at 95 and 278 K. All the Raman lines reported previously (Cherepy et al., 1994; Shreve et al., 1991) are observed, along with a few smaller peaks that can now be identified because of improved data and data analysis methods. Relatively weak P modes at 622, 932, 1011, 1050, 1070, 1099, 1257, and 1278 cm^{-1} are now observed in the 278 K spectrum, while the 128 cm^{-1} feature was found to be better fit by two modes at 127 and 145 cm^{-1}.

The low-frequency region of the P spectrum changes significantly upon cooling to 95 K. The 278 K spectrum contains a pair of strong modes at 127 and 145 cm^{-1}, while the 95 K spectrum has only a weak mode at 132 cm^{-1} in this range. Other differences are much less remarkable: the 70 cm^{-1} peak in the 278 K spectrum is resolved into the 64 and 82 cm^{-1} modes at 95 K, and the 96 cm^{-1} mode shifts to

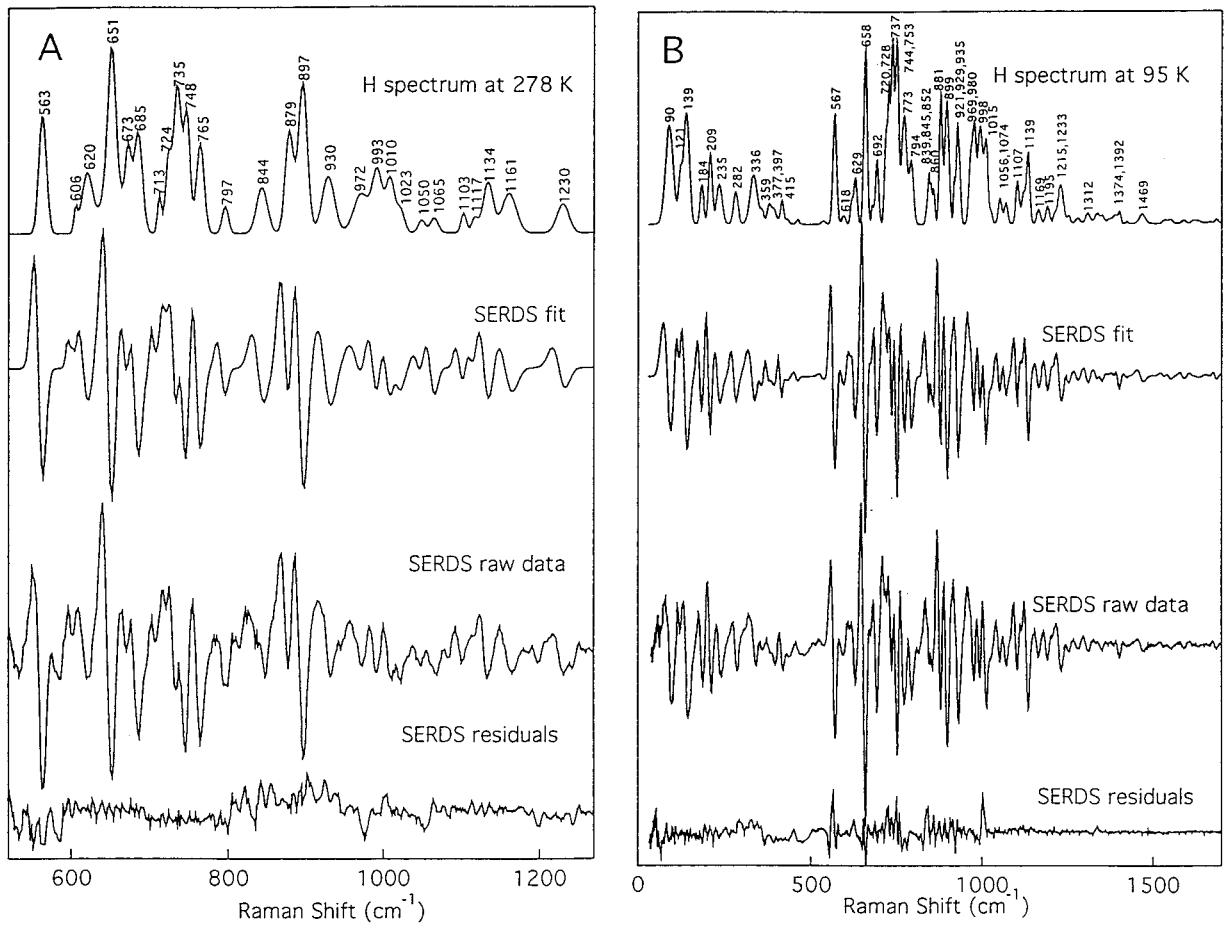

FIGURE 3: (A) Mid-frequency Raman spectrum of H at 278 K obtained using 760 nm excitation ($P = 5-8$ mW). (B) Complete Raman spectrum of H at 95 K obtained using 760 nm excitation ($P = 5-8$ mW). The residuals, the raw data, the least-squares fits to these data, and the spectra generated from the least-squares fits are shown from bottom to top, respectively.

101 cm^{-1}. The 187 cm^{-1} band is resolved into peaks at 168 and 179 cm^{-1} at 95 K. The modes at 262 and 291 cm^{-1} in the 95 K spectrum seem to be present in the SERDS spectrum at 278 K, but were too weak to be fit reliably. Similarly, the 560, 763, 780, 790 cm^{-1}, and other higher frequency modes observed in the 95 K spectrum were not significantly stronger than the noise level in the 278 K spectrum. Weak high frequency modes at 1618, 1650, and 1681 cm^{-1} observed in the low-temperature spectrum correspond to carbonyl stretches that are sensitive to the environment and hydrogen bonding of the dimer.

The spectra in Figure 5 demonstrate that the frequencies and relative intensities in the Raman spectrum of P are independent of excitation wavelength. Figure 5A shows the Raman spectra of P obtained at 278 K with 850, 870, and 890 nm excitation, while Figure 5B shows spectra acquired with the same excitation wavelengths at 95 K. There appear to be some differences in the low-frequency spectral region between the 95 and 278 K spectrum; a reduction in intensity of the 127 and 145 cm^{-1} modes is apparent in all the 95 K spectra.

The Raman excitation profile for the 730 cm^{-1} RC mode is presented in Figure 6. Figure 6A shows the excitation profile at 278 K, while Figure 6B presents the available Raman scattering intensities at 95 K. The absorption spectrum at each temperature is presented for comparison. The absolute intensity of the 730 cm^{-1} RC mode was determined for the P chromophore at 278 and 95 K utilizing 50% ethylene glycol-containing samples. The average absolute Raman cross section measured for P is $(0.53 \pm 0.19) \times 10^{-7}$ Å^2 at 278 K and 850 nm excitation (6 measurements) and $(0.80 \pm 0.24) \times 10^{-7}$ Å^2 at 95 K and 870 nm excitation (6 measurements).[3] Thus, the P Raman cross sections are independent of temperature within their experimental uncertainties. The Raman cross sections of the 731 cm^{-1} mode of B with 800 nm excitation are $(3.74 \pm 0.92) \times 10^{-7}$ Å^2 at 278 K and $(13.6 \pm 2.0) \times 10^{-7}$ Å^2 at 95 K (Cherepy et al., 1997a). Therefore, the absolute Raman cross sections of B are a factor of ~6.5 times larger than the P cross sections, and the difference between the P and B cross sections increases to a factor of ~17 at 95 K.

The Raman cross sections of H at both 278 and 95 K are of approximately the same magnitude as those of B. It is difficult to reference them to the 864 cm^{-1} ethylene glycol mode due to the interference of the H modes which lie between 840 and 880 cm^{-1} as well as the presence of B modes in the 760 nm excited spectrum. To clarify the source of the scattering with excitation below 800 nm, spectra of a dilute 50% ethylene glycol sample were acquired with excitation from 760 to 800 nm (Figure 7). The appearance of the 651 cm^{-1} mode with 760 nm excitation clearly marks it as an H mode, while some of the overlapping modes appearing in the H spectrum, such as the modes in the 730

[3] We have chosen 850 nm excitation at 278 K and 870 nm excitation at 95 K because the P band shifts with temperature and these two points are at the same relative position in the P band at these two temperatures (see Figure 1). The extinction coefficient at 298 K is ~109 000 M^{-1} cm^{-1} at 850 nm, and at 77 K it is ~65 000 M^{-1} cm^{-1} at 870 nm. The absorption spectra do not change significantly between 77 and 95 K nor between 298 and 278 K.

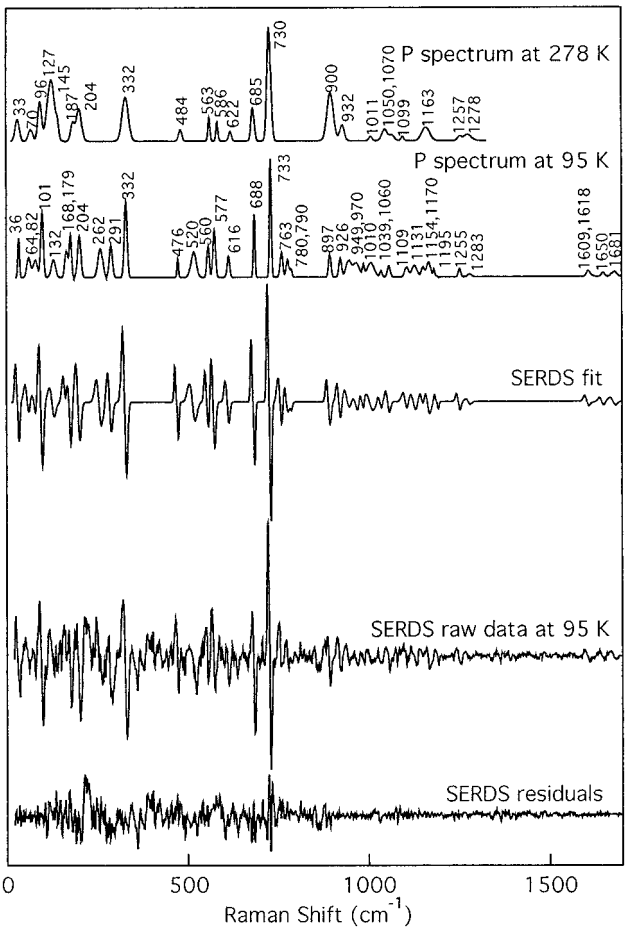

FIGURE 4: Raman spectrum of P at 278 K obtained using 850 nm excitation and the SERDS technique ($P = 5-8$ mW) and the Raman spectrum of P at 95 K obtained using 870 nm excitation ($P = 5-8$ mW). The residuals, the raw data, and the least-squares fits to these data are presented for the 95 K spectrum.

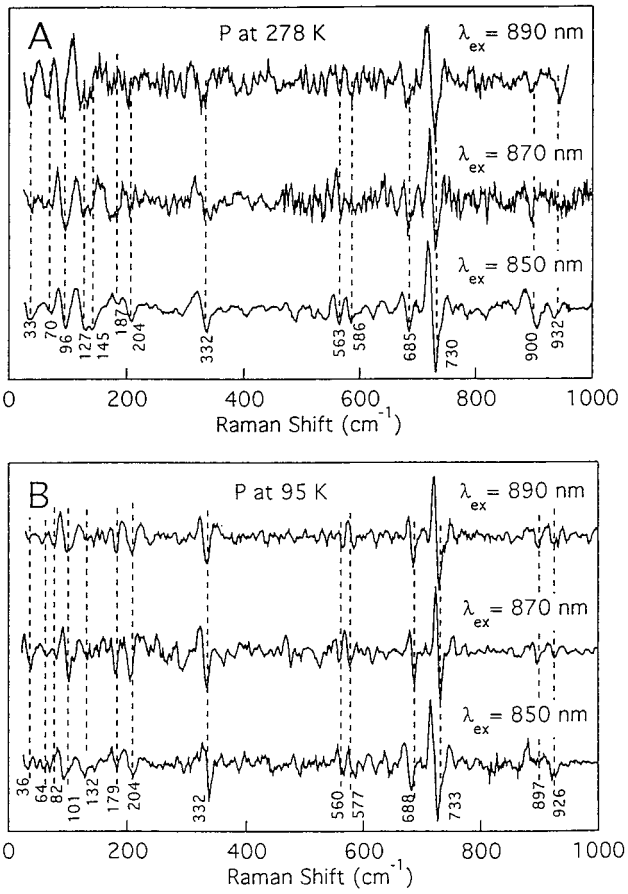

FIGURE 5: (A) P spectra acquired with 850, 870, and 890 nm excitation at 278 K. (B) P spectra acquired with 850, 870, and 890 nm excitation at 95 K. The spectra are scaled to give the same height of the 730 cm^{-1} band.

cm^{-1} region, may have significant contributions from B scattering. The scattering intensity of the 651 cm^{-1} H mode excited at 760 nm is approximately equal to that of the 569 cm^{-1} B mode excited at 800 nm. The Raman scattering of B and H are also of about the same intensity at 95 K (data not shown).

DISCUSSION

Resonance Raman spectra of the B, H, and P chromophores in the bacterial RC have been obtained at 278 and 95 K, revealing information about their vibronic characteristics and excited-state dynamics. The vibrational modes active in the resonance Raman spectra of B and H are coupled to the electronic transitions from which energy transfer to P occurs. Since energy transfer occurs very rapidly, these modes may also directly couple to the energy transfer reaction. Similarly, the resonance Raman spectrum of P reveals the nuclear distortions which couple to the transition from which electron transfer occurs. The Raman spectra of B, H, and P reveal the nuclear motions that are most important to the photophysics of the chromophores. Furthermore, information about excited-state dynamics can be obtained from the resonance Raman cross sections and their temperature dependence.

When we reported the SERDS resonance Raman spectra of B and P at 278 K (Cherepy et al., 1994), we noted significant differences between the B spectrum and that reported earlier (Palaniappan et al., 1992). However, recent low-frequency B and P spectra at 200 K (Palaniappan et al., 1995) agree quite well with the B and P spectra which we originally presented and with the spectra presented here. Similarly, earlier spectra reported of H (Bocian et al., 1987) have now been superseded by improved H Raman spectra acquired at 200 K (Palaniappan et al., 1995). These recent H spectra, acquired with 750 nm excitation, nearly exactly match the spectrum presented in Figure 3B. Palaniappan et al. (1995) find modes at 93, 120, 137, 181, 209, 237, 283, 338, and 357 cm^{-1}, while we report modes at 90, 121, 139, 184, 209, 235, 282, 336, and 359 cm^{-1}. The very close agreement between these studies gives confidence in the accuracy of these spectra and the conclusions derived therefrom.

Spectral Analysis. While the detailed analysis and assignment of the Raman modes is not our primary focus, we will discuss several qualitative features of the spectra. The resonance Raman spectra of B show that the accessory BChls are relatively unperturbed by their inclusion in the protein matrix, since their spectra agree well with the vibrational spectra of BChl in solution, in films and in other photosynthetic proteins. In a previous paper, we compared the B modes with known BChl modes, and were able to assign many of the modes above 600 cm^{-1} (Cherepy et al., 1994; Diers & Bocian, 1995; Johnson & Rubinovitz, 1991; Mattioli et al., 1993; Noguchi et al., 1991; Reddy et al., 1991; Renge et al., 1987; van der Laan et al., 1992). Furthermore, the mode frequencies and relative Raman intensities of B are essentially temperature independent. Good agreement is

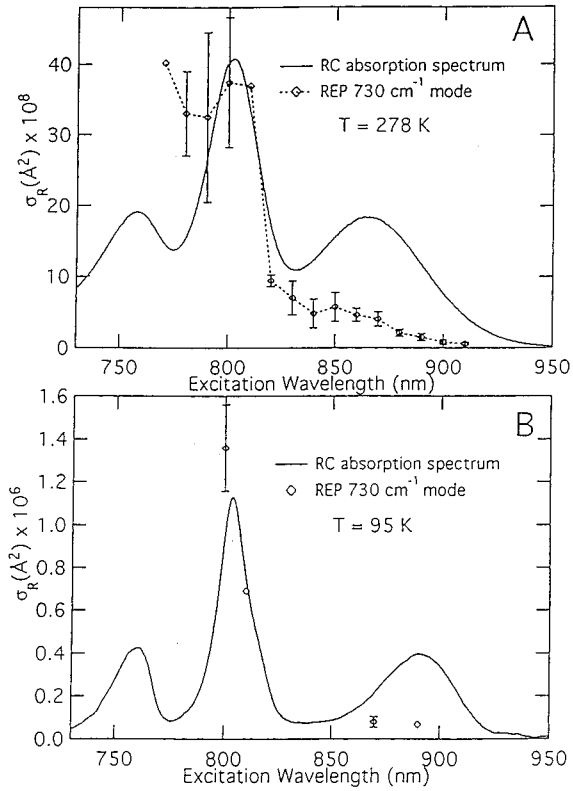

FIGURE 6: (A) Raman excitation profile for the 730 cm^{-1} mode of RCs at 278 K obtained from 1−6 data sets for each excitation wavelength. All intensities measured in the P band are corrected for bleaching as described in text. Excitation powers range from 2 to 6 mW. (B) Raman excitation profile for the 730 cm^{-1} mode of RCs at 95 K. Multiple measurements with 800 and 870 nm excitation at 95 K and their standard deviations are shown. Only one measurement at 810 and 890 nm was made. Excitation powers range from 3 to 6 mW.

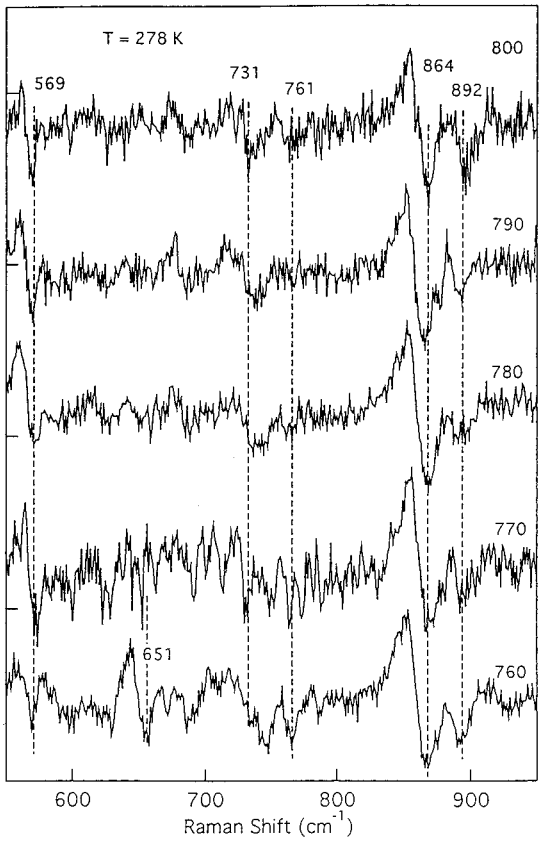

FIGURE 7: Mid-frequency portion of the SERDS spectrum of RCs obtained at 278 K using 760, 770, 780, 790, and 800 nm excitation of a sample in a 50% v/v mixture of buffer and ethylene glycol (o.d. at 800 nm = 0.08). The Raman scattering from H, gauged by the strength of the 651 cm^{-1} mode in the 760 nm spectrum, is about as strong as that from B, gauged by the strength of the 569 cm^{-1} mode with 800 nm excitation. Spectra have been scaled to give a constant 864 cm^{-1} ethylene glycol intensity.

found between the mode patterns of the resonance Raman spectra of H and the room-temperature Fourier transform (FT) Raman spectra of BPheo (Mattioli et al., 1993) and the 5 K site-selection emission features (Renge et al., 1987) of BPheo. This similarity suggests that the BPheo molecules in the RC are not significantly distorted from their conformation *in vitro*.

Comparison of the P and B spectra helps to identify modes that are unique to the protein-bound BChl dimer P and may be significant in its photochemistry. The most obvious differences between P and B are in the low-frequency region. At 278 K there are relatively strong modes at ∼33, 70, 96, 127, and 145 cm^{-1} in the P spectrum, while in B this region has only a weak mode at 117 cm^{-1} and possibly weak modes at ∼60 and ∼85 cm^{-1}. The new low-frequency modes appearing in the P spectrum are likely to have some intradimer character, and thus may be mechanistically implicated in the electron transfer from P*.

The most important temperature-dependent changes in the P spectrum also occur in the low-frequency region. The 278 K spectrum is dominated by a pair of strong modes at 127 and 145 cm^{-1}, which are replaced in the 95 K spectrum by a weak mode at 132 cm^{-1}. Furthermore, the 187 cm^{-1} mode at 278 K seems to shift and split into the 168 and 179 cm^{-1} modes at 95 K. This temperature dependence supports the suggestion that these modes have significant intradimer character. When the temperature is decreased, there is a red shift of the absorption spectrum of P (see Figure 1). This may in part be due to the two BChl molecules of the dimer coming closer together, thus changing their excitonic coupling, shifting the lower exciton transition to lower energy (Thompson et al., 1990, 1991). A change in intermolecular distance in the dimer with temperature would not be surprising. It has been shown that the P band shifts to the red when the pressure is increased and it is likely that reduction in temperature has a similar effect (Small, 1995). It is thus reasonable to conclude that the changes in the low-frequency P spectra are induced by temperature-dependent changes in the coupling of the two P chromophores.

In exploring the implications of the enhanced low-frequency modes on the electron transfer dynamics, it is very helpful to compare the resonance Raman spectrum of P with the power spectrum generated from the oscillations superimposed on the femtosecond stimulated and spontaneous emission of P*. The Raman modes report on the motions coupled to the P transition, while the oscillations in the femtosecond spectra correspond to coherent nuclear motions occurring in the excited state of P which decay on the time scale of electron transfer. Since the vibrational frequencies and relative intensities of the Raman spectrum of P are in very good agreement with the power spectrum of the femtosecond oscillations, it is likely that they correspond to the same motions. The oscillations in the stimulated emission of P* have been measured at 10, 100, and 298 K (Vos et al., 1994a,b). Oscillations in the spontaneous emission have been measured at 82 K (Stanley & Boxer, 1995). Low-frequency oscillations in the 298 K stimulated emission have frequencies of 30, 84, 145, and 192 cm^{-1},

which nicely match the 278 K Raman modes at 33, 70, 96, 127/145, and 187/204 cm^{-1}. The 10 and 100 K stimulated emission oscillation frequencies at 15, 69, 92, 122, 153, and 191 cm^{-1} are generally in very good agreement with our P modes at 36, 64/82, 101, 132, 168/179, and 204 cm^{-1}. The only difference is that the low-temperature Raman spectrum contains only a weak 132 cm^{-1} mode in the 127−145 cm^{-1} range. Intriguingly, Vos et al. (1994a) report that the ∼127 cm^{-1} oscillation undergoes more rapid vibrational dephasing (∼200 fs) than the other modes (∼500 fs), suggesting that this mode may have unique characteristics, such as a change in frequency or anharmonicity in the excited state. In contrast, the 82 K spontaneous fluorescence from P exhibits an intense Fourier component at ∼100 cm^{-1} and lacks a strong ∼127 cm^{-1} mode; this behavior is more consistent with our 95 K Raman spectrum. To further explore the temperature dependence of the ∼127 cm^{-1} Raman mode, we acquired a spectrum of P at 150 K. This spectrum also lacks a strong feature in the 120−150 cm^{-1} region, similar to the 95 K spectrum in Figure 4B. Thus, the weakening of the 127 cm^{-1} mode of P on cooling from 278 to 95 K and the appearance of the strong 101 cm^{-1} mode is in agreement with the spontaneous emission oscillations. Conversely, the stimulated emission oscillations found by Vos et al. (1994a,b) at 10, 100, and 298 K are consistently dominated by the 122/153 cm^{-1} modes. These results indicate that there is a significant temperature-dependent difference in the nuclear motions coupled to the optical excitation of P.

Absolute Raman Cross Sections. A surprising feature of the RC is the difference in magnitude of the Raman cross sections between the chromophores (Cherepy et al., 1994). The ubiquitous 730 cm^{-1} mode provides a good basis for comparison. The cross sections for the 730 cm^{-1} mode of P are a factor of ∼6.5 times smaller than the B cross sections at 278 K, but the H cross sections are similar to those of B at both 95 and 278 K. While the P cross sections are nearly temperature independent, the B and H cross sections increase by a factor of ∼3−4 when the temperature is reduced to 95 K. *At 95 K, the P scattering intensity is ∼17-fold weaker than that of B and H.*

The absolute Raman intensities of B measured with 800 nm excitation increase by a factor of ∼4 when the temperature is decreased from 278 to 95 K. Since the population lifetime for B corresponds to the ∼100 fs energy transfer time from B* to P (Jia et al., 1995; Martin et al., 1986; Stanley et al., 1996) and is only slightly temperature dependent, the strong temperature dependence of the Raman cross sections of B must be due to pure dephasing arising from low-frequency protein/solvent modes coupling to the B transitions which become thermally activated as the temperature increases. In the absence of the specifics of available bath modes and coupling strengths, we have modeled the pure dephasing with a Gaussian homogeneous line width that increases with temperature. A full analysis of the temperature dependence of the scattering of B as well as a model for its vibronic properties can be found in Cherepy et al. (1997a).

Since the Raman cross sections of H are of similar magnitude and display similar temperature dependence to those of B, it is likely that the electronic and nuclear dynamics of H resemble those of B. The strong temperature dependence of the H cross sections also indicates that there are significant pure dephasing contributions at room temperature. The energy transfer from H* to P is about 2 times slower than the energy transfer from B* to P (Stanley et al., 1996). It is unclear how energy transfer from H proceeds. The depopulation of the H excited state may be due to energy transfer to B, or direct energy transfer to P may occur. Modeling of the Raman excitation profiles of H in conjunction with its absorption spectrum utilizing the spectra and intensities presented here may lead to better understanding of the excited-state dynamics of H.

The Raman cross sections of P are temperature independent and weak, suggesting either rapid temperature-independent vibronic dephasing or that a more complicated description of its excited state may be necessary (Cherepy et al., 1997b). If it is assumed that the excited state of P is a simple exciton state and that the P band is broadened through coupling to its own molecular modes and to bath modes, then a large homogeneous line width (735 cm^{-1} full width at half-maximum, corresponding to a dephasing time of 24 fs) is necessary to simultaneously fit the Raman cross sections and the P absorption band (Cherepy et al., 1997b). However, modeling of the hole-burning spectrum of P using a simple single excited state potential surface indicates strong coupling and a slow dephasing time at low temperature, in contradiction with the weak electron−nuclear coupling suggested by the modeling of the Raman cross sections. The small Raman cross sections may also be explained by a model such as that proposed by Friesner and co-workers, in which the P band is broadened through the coupling of the lower-exciton state to a charge transfer state (Lathrop & Friesner, 1994). In this model, the 860 nm band corresponds to a state containing an admixture of a lower exciton state and a dark charge transfer state. A different formulation of this type of model has been advanced by Small et al. (1995), where the lower exciton P state is coupled to a quasi-degenerate $P^+B_A^-$ state. Either of these proposed excited-state structures would allow the modeling of the broad P band with weak electron−nuclear coupling within the exciton state, but strong effective electron−nuclear coupling resulting from the coupling between the exciton state and a charge transfer state. While this approach has been shown to reproduce hole-burning results (Lathrop & Friesner, 1994), the implications for Raman cross section calculations have not been explored in detail.

Since the Raman cross sections of P are approximately temperature independent, this may be an indication that the excited state dephasing time of P is very rapid. The overall electronic dephasing time is comprised of contributions from population relaxation and pure dephasing. Temperature-independent dephasing is consistent with a population relaxation-controlled process. Coupling of multiple excited states could also lead to temperature-independent dephasing, similar to that observed for fast population relaxation. Schomacker and Champion (1989) examined the temperature dependence of the Raman spectrum of ferrocytochrome *c* and found little variation of the Raman cross sections as a result of the rapid temperature-independent population relaxation time of ∼14 fs. Since pure dephasing processes generally result from coupling to low-frequency solvent modes and thus are temperature dependent, a dephasing time which is not temperature dependent probably contains no contributions from pure dephasing. In contrast, the room-temperature population lifetime of B*, due to energy transfer to P, is ∼100 fs (Jia et al., 1995; Martin et al., 1986). In this somewhat longer time, our data show that pure dephasing from the protein solvent can become significant, causing the

Raman cross sections to have a strong temperature dependence.

In conclusion, the vibronic properties of the chromophores in the bacterial reaction center have been characterized. Temperature-dependent changes in the low-frequency spectrum of P suggest that there is a temperature dependence of the vibronic structure of P. Strong temperature dependence of the Raman cross sections of B and H indicates that there is significant pure dephasing due to low-frequency protein modes, while the weak temperature-independent cross sections of P are consistent with a fast, bath-independent dephasing time. The Raman spectra of B and H identify the modes that may be coupled to the energy transfer from B and H. The modes observed in the resonance Raman spectrum of P are in good agreement with the vibrational oscillations that modulate the emission from the excited state of P and may be coupled to electron transfer. The properties measured in these spectra may be used to detail the nuclear distortions that occur upon chromophore excitation and to derive information on vibronic relaxation processes. Quantitative modeling of the Raman and absorption spectra of both B (Cherepy et al., 1997a) and P (Cherepy et al., 1997b) will be presented elsewhere.

SUPPORTING INFORMATION AVAILABLE

Relative mode intensities and frequencies for the B, H and P spectra in Tables 1, 2, and 3. Table 3 compares our H Raman spectra with the available vibrational spectra of BPheo (5 pages). Ordering information is given on any current masthead page.

REFERENCES

Bocian, D. F., Boldt, N. J., Chadwick, B. W., & Frank, H. A. (1987) *FEBS Lett. 214*, 92−96.

Boxer, S. G., Goldstein, R. A., Lockhart, D. J., Middendorf, T. R., & Takiff, L. (1989) *J. Phys. Chem. 93*, 8280−8294.

Cherepy, N. J., Shreve, A. P., Moore, L. J., Boxer, S. G., Franzen, S., & Mathies, R. A. (1994) *J. Phys. Chem. 98*, 6023−6029.

Cherepy, N. J., Holzwarth, A. R., & Mathies, R. A. (1995) *Biochemistry 34*, 5288−5293.

Cherepy, N. J., Du, M., Holzwarth, A. R., & Mathies, R. A. (1996) *J. Phys. Chem. 100*, 4662−4671.

Cherepy, N. J., Shreve, A. P., Moore, L. J., Boxer, S. G., & Mathies, R. A. (1997a) *J. Phys. Chem. B 101*, 3250−3260.

Cherepy, N. J., Shreve, A. P., Moore, L. J., Franzen, S., Boxer, S. G., & Mathies, R. A. (1997b) (in preparation).

Diers, J. R., & Bocian, D. F. (1995) *J. Am. Chem. Soc. 117*, 6629−6630.

Fleming, G. R., & van Grondelle, R. (1994) *Phys. Today 47*, 48−55.

Friesner, R. A., & Won, Y. (1989) *Biochim. Biophys. Acta 977*, 99−122.

Jia, Y., Jonas, D. M., Joo, T., Nagasawa, Y., Lang, M. J., & Fleming, G. R. (1995) *J. Phys. Chem. 99*, 6263−6266.

Johnson, C. K., & Rubinovitz, R. (1991) *Spectrochim. Acta 47A*, 1413−1421.

Johnson, S. G., Tang, D., Jankowiak, R., Hayes, J. M., Small, G. J., & Tiede, D. M. (1989) *J. Phys. Chem. 93*, 5953−5957.

Kirmaier, C., & Holten, D. (1987) *Photosynth. Res. 13*, 225−260.

Klevanik, A. V., Ganago, A. O., Shkuropatov, A. Ya., & Shuvalov, V. A. (1988) *FEBS Lett. 237*, 61−64.

Lathrop, E. J. P., & Friesner, R. A. (1994) *J. Phys. Chem. 98*, 3056−3066.

Loppnow, G. R., & Mathies, R. A. (1988) *Biophys. J. 54*, 35−43.

Martin, J.-L., Breton, J., Hoff, A. J., Migus, A., & Antonetti, A. (1986) *Proc. Natl. Acad. Sci. U.S.A. 83*, 957−961.

Mathies, R., & Yu, N.-T. (1978) *J. Raman Spectrosc. 7*,349−352.

Mathies, R., Oseroff, A. R., & Stryer, L. (1976) *Proc. Natl. Acad. Sci. U.S.A. 73*,1−5.

Mattioli, T. A., Hoffmann, A., Sockalingum, D. G., Schrader, B., Robert, B., & Lutz, M. (1993) *Spectrochim. Acta 49A*, 785−799.

Mattioli, T. A., Williams, J. C., Allen, J. P., & Robert, B. (1994) *Biochemistry 33*, 1636−1643.

Meech, S. R., Hoff, A. J., & Wiersma, D. C. A. (1985) *Chem. Phys. Lett. 121*, 287−292.

Middendorf, T. R., Mazzola, L. T., Gaul, D. F., Schenck, C. C., & Boxer, S. G. (1991) *J. Phys. Chem. 95*, 10142−10151.

Morikis, D., Li, P., Bangcharoenpaurpong, O., Sage, J. T., & Champion, P. M. (1991) *J. Phys. Chem. 95*, 3391−3398.

Myers, A. B., Harris, R. A., & Mathies, R. A. (1983) *J. Chem. Phys. 79*, 603−613.

Noguchi, T., Furukawa, Y., & Tasumi, M. (1991) *Spectrochim. Acta 47A*, 1431−1440.

Okamura, M., Isaacson, R. A., & Feher, G. (1975) *Proc. Natl. Acad. Sci. U.S.A. 72*, 3491−3495.

Palaniappan, V., Aldema, M. A., Frank, H. A., & Bocian, D. F. (1992) *Biochemistry 31*, 11050−11058.

Palaniappan, V., Schenck, C. C., & Bocian, D. F. (1995) *J. Phys. Chem. 99*, 17049−17058.

Phillips, D. L., & Myers, A. B. (1991) *J. Chem. Phys. 95*, 226−243.

Reddy, N. R. S., Small, G. J., Seibert, M., & Picorel, R. (1991) *Chem. Phys. Lett. 181*, 391−399.

Rees, D. C., Komiya, H., Yeates, T. O., Allen, J. P., & Feher, G. (1989) *Annu. Rev. Biochem. 58*, 607−633.

Renge, I., Mauring, K., & Avarmaa, R. (1987) *J. Luminescence 37*, 207−214.

Schenck, C. C., Blankenship, R. E., & Parson, W. W. (1982) *Biochim. Biophys. Acta 680*, 44−59.

Schomacker, K. T., & Champion, P. M. (1989) *J. Chem. Phys. 90*, 5982−5993.

Shreve, A. P., Cherepy, N. J., Franzen, S., Boxer, S. G., & Mathies, R. A. (1991) *Proc. Natl. Acad. Sci. U.S.A. 88*, 11207−11211.

Shreve, A. P., Cherepy, N. J., & Mathies, R. A. (1992) *Appl. Spectrosc. 46*, 707−711.

Small, G. J. (1995) *Chem. Phys. 197*, 239−257.

Stanley, R. J., & Boxer, S. G. (1995) *J. Phys. Chem. 99*, 859−863.

Stanley, R. J., King, B., & Boxer, S. G. (1996) *J. Phys. Chem. 100*, 12052−12059.

Sue, J., & Mukamel, S. (1988) *J. Chem. Phys. 88*, 651−665.

Thompson, M. A., Zerner, M. C., & Fajer, J. (1990) *J. Phys. Chem. 94*, 3820−3828.

Thompson, M. A., Zerner, M. C., & Fajer, J. (1991) *J. Phys. Chem. 95*, 5693−5700.

van der Laan, H., Smorenburg, H. E., Schmidt, Th., & Volker, S. (1992) *J. Opt. Soc. Am. B 9*, 931−940.

Vos, M. H., Lambry, J.-C., Robles, S. J., Youvan, D. C., Breton, J., & Martin, J.-L. (1991) *Proc. Natl. Acad. Sci. U.S.A. 88*, 8885−8889.

Vos, M. H., Rappaport, F., Lambry, J.-C., Breton, J., & Martin, J.-L. (1993) *Nature 363*, 320−325.

Vos, M. H., Jones, M. R., Hunter, C. N., Breton, J., Lambry, J.-C., & Martin, J.-L. (1994a) *Biochemistry 33*, 6750−6757.

Vos, M. H., Jones, M. R., Hunter, C. N., Breton, J., & Martin, J.-L. (1994b) *Proc. Natl. Acad. Sci. U.S.A. 91*, 12701−12705.

Zankel, K., Reed, D., & Clayton, R. (1968) *Proc. Natl. Acad. Sci. U.S.A. 61*, 1243−1249.

BI970024R